ADVANCED MATERIALS

Supporting Information

for *Adv. Mater.,* DOI: 10.1002/adma.202106068

3D Printing of Superhydrophobic Objects with Bulk Nanostructure

*Zheqin Dong, Maja Vuckovac, Wenjuan Cui, Quan Zhou, Robin H. A. Ras, and Pavel A. Levkin**

Supporting Information

3D printing of superhydrophobic objects with bulk nanostructure

*Zheqin Dong, Maja Vuckovac, Wenjuan Cui, Quan Zhou, Robin H. A. Ras and Pavel A. Levkin**

Dr. Z. Dong, Prof. P. A. Levkin
Institute of Biological and Chemical Systems – Functional Molecular Systems (IBCS-FMS)
Karlsruhe Institute of Technology (KIT)
Hermann-von-Helmholtz-Platz 1, Eggenstein-Leopoldshafen 76344, Germany
E-mail: levkin@kit.edu

Dr. M. Vuckovac, Prof. R. H. A. Ras
Department of Applied Physics
Aalto University School of Science
02150 Espoo, Finland
Prof. R. H. A. Ras
Department of Bioproducts and Biosystems
Aalto University School of Chemical Engineering
02150 Espoo, Finland.

Dr. W. Cui, Prof. Q. Zhou
Department of Electrical Engineering and Automation
Aalto University School of Electrical Engineering
02150 Espoo, Finland

This PDF file includes
Tables S1 to S4
Figures S1 to S5
Supplementary Discussion 1
Experimental section
Captions for Videos S1 to S8

Table S1. Physical properties of nanoporous cubes (5 × 5 × 5 mm^3) 3D-printed from inks containing BA as the monomer, EDMA as the crosslinker, with different porogen composition and ratios.

Ink Number	BA (wt%)	EDMA (wt%)	1-Decanol (wt%)	Cyclo hexanol (wt%)	Average globular size (nm)	Porosity (%)	θ^*_{adv} (°)	θ^*_{rec} (°)	$\Delta\theta^*$ (°)	Compression strength (MPa)
BA-1	30	20	50	0	637 ± 44	39.1 ± 1.5	164.5 ± 1.2	151.4 ± 1.3	13.1 ± 2.0	7.6 ± 0.3
BA-2	30	20	25	25	201 ± 46	36.3 ± 3.5	161.3 ± 1.2	127.9 ± 2.4	33.5 ± 1.2	10.9 ± 1.0
BA-3	30	20	0	50	57 ± 10	35.3 ± 1.2	146.2 ± 2.5	88.0 ± 6.9	58.2 ± 6.7	20.1 ± 0.6
BA-4	21	14	32.5	32.5	452 ± 61	47.4 ± 0.7	163.3 ± 1.2	154.7 ± 2.0	8.5 ± 1.1	1.2 ± 0.1
BA-5	39	26	17.5	17.5	60 ± 9	22.2 ± 0.8	158.5 ± 2.8	100.9 ± 3.6	57.6 ± 3.2	27.5 ± 1.7

Table S2. Physical properties of nanoporous cubes (5 × 5 × 5 mm^3) 3D-printed using inks containing LA as the monomer, EDMA as the crosslinker, with different porogen composition and ratios.

Ink Number	LA (wt%)	EDMA (wt%)	1-Decanol (wt%)	Cyclo hexanol (wt%)	Average globular size (nm)	Porosity (%)	θ^*_{adv} (°)	θ^*_{rec} (°)	$\Delta\theta^*$ (°)	Compression strength (MPa)
LA-1	30	20	50	0	740 ± 99	33.4 ± 2.1	164.1 ± 0.4	150.4 ± 1.0	13.6 ± 1.3	2.1 ± 0.1
LA-2	30	20	25	25	130 ± 25	30.7 ± 1.4	159.1 ± 1.5	130.1 ± 1.8	29.1 ± 2.4	7.1 ± 0.1
LA-3	30	20	0	50	51 ± 11	31.4 ± 2.3	151.9 ± 1.9	109.1 ± 4.2	42.7 ± 5.0	9.8 ± 0.8
LA-4	21	14	32.5	32.5	430 ± 17	43.6 ± 1.1	162.7 ± 1.5	153.8 ± 1.3	8.9 ± 0.3	0.9 ± 0.1
LA-5	39	26	17.5	17.5	51 ± 7	21 ± 1.8	150.4 ± 1.0	116.8 ± 5.2	33.6 ± 4.2	14.6 ± 2.4

Table S3. Physical properties of nanoporous cubes (5 × 5 × 5 mm^3) 3D-printed using inks containing HFBA and BA (1:1 w:w) as the monomer, EDMA as the crosslinker, with different porogen composition and ratios.

Ink Number	HFBA (wt%)	BA (wt%)	EDMA (wt%)	1-Decanol (wt%)	Cyclo hexanol (wt%)	Average globular size (nm)	Porosity (%)	θ^*_{adv} (°)	θ^*_{rec} (°)	$\Delta\theta^*$ (°)	Compression strength (MPa)
HFBA-BA-1	15	15	20	50	0	993 ± 48	34.0 ± 1.7	164.7 ± 1.3	155.2 ± 0.5	9.5 ± 1.5	2.5 ± 0.1
HFBA-BA-2	15	15	20	25	25	325 ± 21	33.8 ± 1.2	164.9 ± 0.6	152.0 ± 2.5	12.9 ± 2.9	9.9 ± 0.5
HFBA-BA-3	15	15	20	0	50	87 ± 14	32.3 ± 0.9	162.5 ± 1.0	150.7 ± 1.0	11.8 ± 1.5	14.9 ± 0.7
HFBA-BA-4	10.5	10.5	14	32.5	32.5	410 ± 32	44.8 ± 2.4	163.9 ± 1.5	155.5 ± 1.8	8.4 ± 1.8	1.4 ± 0.2
HFBA-BA-5	19.5	19.5	26	17.5	17.5	86 ± 10	20.6 ± 1.2	159.0 ± 1.2	135.8 ± 6.0	23.2 ± 5.4	28.0 ± 0.8

Table S4. Water contact angles of non-porous cubes (5 × 5 × 5 mm^3) 3D-printed using inks without porogens.

Ink number	BA (wt%)	LA (wt%)	HFBA (wt%)	EDMA (wt%)	θ^*_{st} (°)	θ^*_{adv} (°)	θ^*_{rec} (°)
BA	60	-	-	40	73.6 ± 0.3	84.7 ± 0.4	66.8 ± 0.4
LA	-	60	-	40	79.7 ± 0.5	92.3 ± 0.3	70.2 ± 0.8
HFBA-BA	30	-	30	40	90.1 ± 0.3	100.7 ± 0.4	81.9 ± 0.3

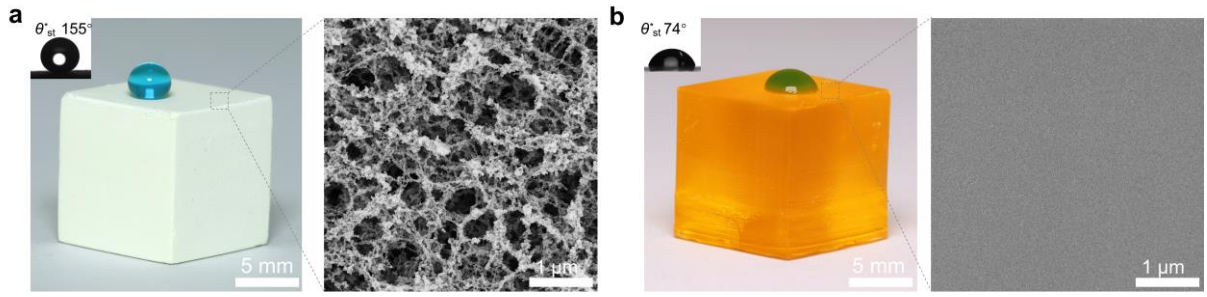

Figure S1. Photographs of dyed water droplets on (a) nanoporous cube printed using a phase separating ink with porogens (30 wt% BA, 20 wt% EDMA, 50 wt% 1-decanol), and (b) non-porous cube an ink without porogens (60 wt% BA, 40 wt% EDMA), with an insert showing the measured static water contact angle (θ^*_{st}). The SEM images on the right show their distinct surface morphology.

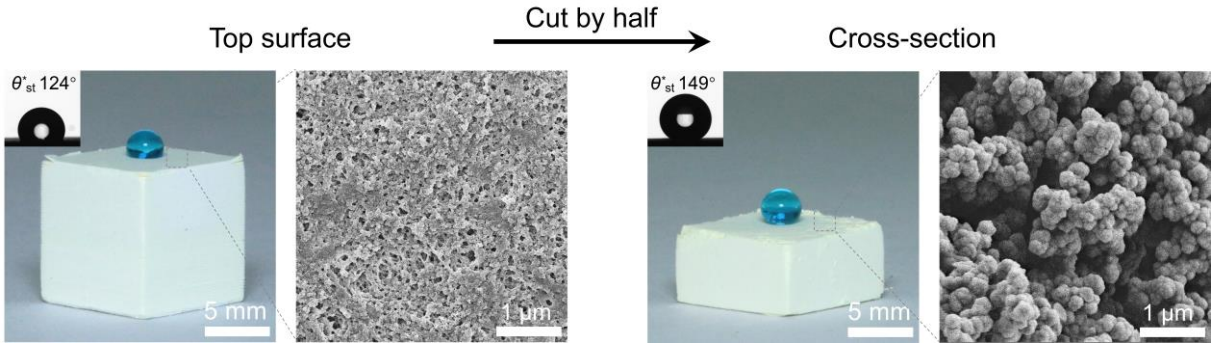

Figure S2. Photographs and SEM images of a 3D-printed nanoporous cube after drying in air. The insets show the corresponding static water contact angle (θ^*_{st}).

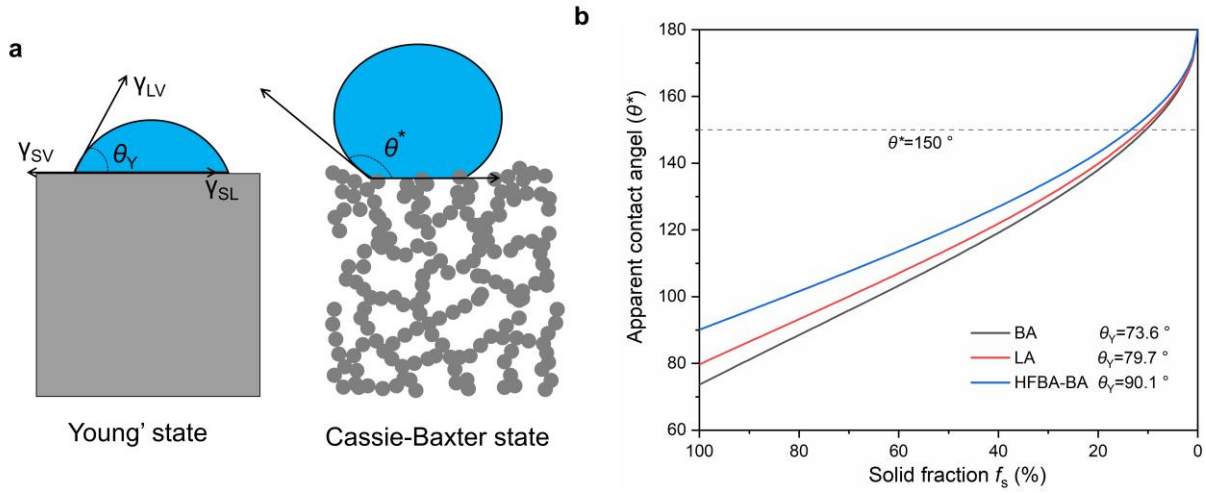

Figure S3. a) Schematic models showing a liquid droplet sitting on an ideally smooth surface (Young's state) and a nanoporous surface (Cassie-Baxter state). b) Relation between apparent contact angle (θ*) and solid fraction f_s for ideal Cassie-state droplets with different Young's contact angles (θ_Y).

Supplementary Discussion 1:

The 3D-printed non-porous objects possess a relatively smooth surface (as shown in Figure S1b). Ideally, the contact angle of a droplet on such a smooth surface follows the Young's equation (Figure S3a):

$$\cos\theta_Y = \frac{\gamma_{SV} - \gamma_{SL}}{\gamma_{LV}} \quad (1)$$

where θ_Y is the Young's contact angle, γ_{SV}, γ_{SL}, γ_{LV} represent the surface tension between a solid–liquid, solid–vapor, and liquid–vapor, respectively. θ_Y only depends on the free surface energy of a material, therefore is also referred to materials' intrinsic contact angle. It has been reported that the maximum value θ_Y of water could only reach about 120 °, on a CF_3-terminated low-energy surface.[1] This means that superhydrophobicity cannot be achieved by surface chemistry alone.

The nanoporous structure, however, can suspend the liquid droplet in a Cassie-Baxter state (Figure S3a). In this state, the droplet sits on a composite air-solid composite interface, and the apparent contact angle can be calculated as follows:

$$\cos\theta^* = -1 + f_s\,(1 + \cos\theta_Y) \quad (2)$$

where f_s is the liquid-solid contact fraction, i.e., the proportion of liquid-solid contact area to the projected area of the entire composite interface.

The influence of f_s on the apparent contact angle θ^* is demonstrated by plotting Eq. 2 with different intrinsic contact angles (θ_Y). Evidently, the apparent contact angle θ^* is significantly increased with a decrease of f_s, which explains the high θ^* achieved on the 3D-printed nanoporous objects (Figure S3b).

On the other hand, at the same liquid-solid fraction, higher intrinsic contact angle (θ_Y) gives a higher apparent contact angle θ^*. Therefore, the nanoporous objects printed from HFBA-BA monomer (with highest θ_Y) demonstrate the highest apparent contact angle θ^* for the same level of porosity and globular size (Figure 2a-b).

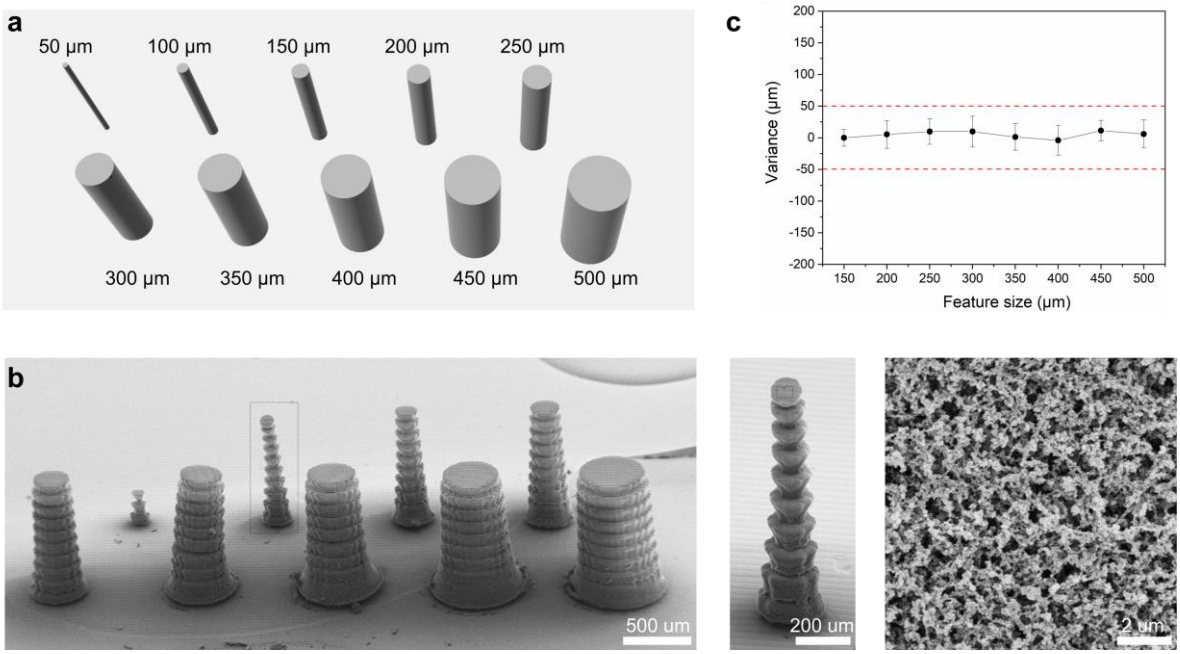

Figure S4. a) 3D design of an array of pillars with different diameters (height 1 mm). b) SEM micrographs of the 3D-printed pillar array with different magnifications. c) Measured deviation between the designed and printed pillar diameter.

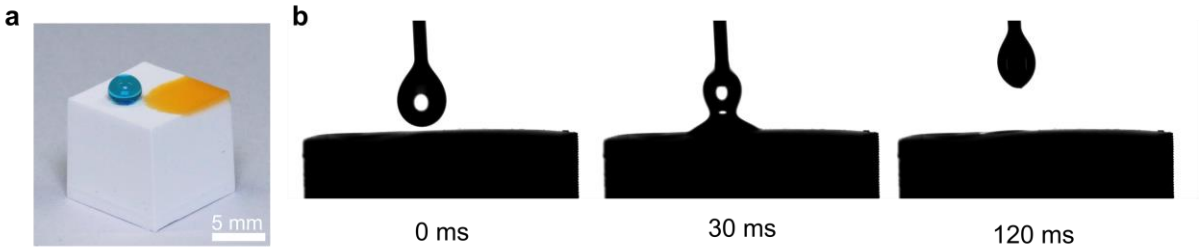

Figure S5. a) Photograph showing a water droplet (blue) and an oil droplet (red) on the 3D-printed bulk superhydrophobic cube. b) Snapshots of a video showing the fast permeation of oil droplets into the cube.

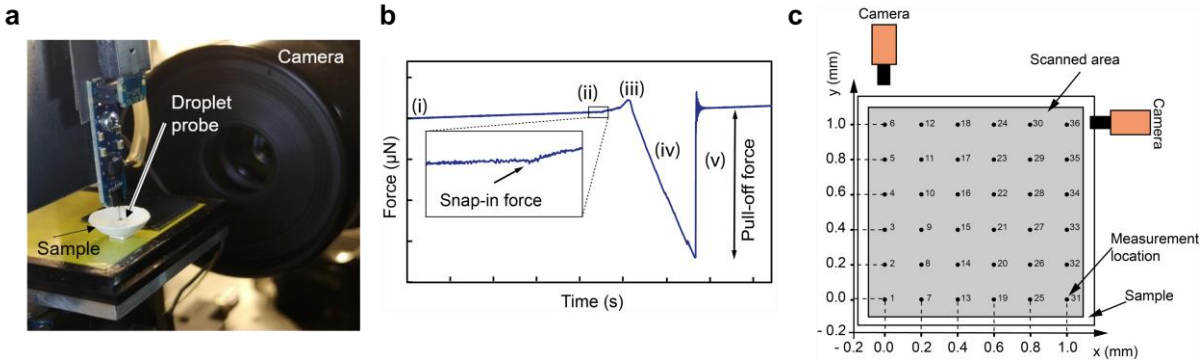

Figure S6. a) Photograph of the SDAM apparatus. b) Typical force curve given by SDAM. c) Schematic showing the multi-points measured in a 1×1 mm^2 square to obtain a force map.

Experimental Section:

Materials and Chemicals: Irgacure 819 was purchased from VWR and all the other chemicals were purchased from Sigma-Aldrich and used without further purification.

Ink Preparation: The inks used for DLP 3D printing were prepared by mixing a certain amount of monomers, porogens, photoinitiators and light-absorbing dyes. The inks were sonicated for 30 min to obtain a clear and homogenous solution, and then stored in fridge at 4 °C before usage. Ink compositions were defined by the mass fraction (wt%) of their components (Table S1 to S3). For all the inks, Irgacure 819 was used as photoinitiator at 2 wt% (relative to the reactive monomer content), and Sudan I was used as light-absorbing dye at 0.005 wt% (relative to the total ink content) to achieve reasonable vertical resolution.

3D Printing: A commercial desktop DLP printer (Miicraft Prime 110) was used for the 3D printing experiments. The printer is based on a LED projector (385 nm) with an intensity of 1.0 mW cm^{-2} at the vat and a XY resolution of 40 μm. The build area is 116 mm × 62 mm × 12 mm and the layer thickness can be adjusted from 5 to 500 μm. The prepared ink solution (~30 mL) was poured into the resin tank. Then the 3D printing started by irradiating the ink with a pre-determined cure time for a given layer thickness (100 μm). After printing, the 3D-printed objects were carefully separated from the build platform and then immersed in acetone for 24 h to remove the unreacted monomers and porogens.

Supercritical Drying: After 3D printing, supercritical drying was used to avoid the collapse of the 3D-printed nanoporous structures. The printed objects immersed in acetone were first transferred to the chamber of the supercritical apparatus (Leica EM CPD030). Then, acetone was replaced by liquid CO_2 by repeatedly flushing with liquid CO_2 and releasing the acetone. Subsequently, the chamber temperature and pressure were increased to 35 °C and 90 bar to maintain the CO_2 in supercritical condition. Finally, the chamber pressure was gradually dropped to atmospheric pressure to release the CO_2. The entire supercritical drying process took about 40 minutes.

Sample Characterization: The porous structure of the 3D-printed objects was characterized by a scanning electron microscope (Zeiss LEO 1530) at an operating voltage of 5 kV. Prior to the SEM measurements, the samples were coated with a 7 nm thick platinum layer. The polymer globular size was measured from the SEM images manually using Image J. The average globule size and the standard deviations are based on 150 measurements. The porosity was measured from the SEM images using the Otsu's method in Image J.

The mechanical property of the 3D-printed objects was tested using a universal testing machine (Shimadzu, AGS-X). The specimen ($5\times5\times5$ mm^3 by design) was compressed in the Z-direction at a rate of 0.5 mm/min until sample fracture was detected in the stress-strain plot. The strength at the fracture point was determined as the compression strength.

The water contact angles of the samples were characterized by a contact angle goniometer (Krüss, DSA 25). Static contact angle (θ^*_{st}) was measured with a 5 µL water droplet and sliding angle was measured at a tilt speed of 60 °/min. Advancing contact angle (θ^*_{adv}) and receding contact angle (θ^*_{rec}) were measured by adding and retracting the liquid at a rate of 0.1 µL/s, respectively.

Scanning Droplet Adhesion Microscopy (SDAM): The wetting property of the 3D-printed superhydrophobic bowls was characterized by SDAM. The detailed description of the SDAM apparatus was provided in the work by V. Liimatainen et al.[2] Briefly, the apparatus was made up of a vertically mounted force sensor with a liquid probe (e.g. water droplet), a multi-axis sample stage, and two cameras mounted at 90° for visualization (Figure 3c and Figure S6a).

For single-point measurement, the sample was first moved to approach the water droplet (1.5 µL) at 5 µm/s and then retracted at 10 µm/s. A typical force curve is shown in Figure S6b: the snap-in force corresponds to the first contact between the droplet and the surface, and the pull-off force corresponds to droplet detachment from the surface.

The pull-off force maps were obtained on the inner center area of the 3D-printed bowls by scanning an area of 1×1 mm^2 with 200 μm resolution. The measurement started by performing a single point measurement in location 1, and then the droplet was refilled to keep constant droplet volume, followed by neutralization to remove any charge. The sample then moves for 200 μm to location 2 where the next single measurement was done, and this process was repeated for remained 34 locations (Figure S6c).

Sandpaper abrasion test: The bulk superhydrophobic brick was 3D-printed using an ink with porogens (HFBA-BA-3). To prepare the post-modified superhydrophobic brick, a non-porous brick was first printed using an ink with the same monomer but without porogen, followed by treatment with a commercial superhydrophobic spray coating (Neverwet). The two superhydrophobic bricks were placed on a sandpaper under a weight of 100 g (equivalent to a pressure of ~10 kPa), and then moved 10 cm across the sandpaper. The abrasion was repeated for 40 cycle, and the static water contact angle (θ_{st}) and water sliding angle (α) on the brick surface were measured after each cycle.

Microfluidic experiments: The porous superhydrophobic channel was 3D-printed using the BA-1 ink. The transparent superhydrophobic cover was printed using poly(ethylene glycol) diacrylate (Mw 250, a widely used resin for DLP printing of microfluidics), [3-5] followed by treatment with a transparent superhydrophobic coating (Glaco). Sealing the superhydrophobic channel and cover with a cyanoacrylate adhesive afforded the microfluidic device (Figure 5a). The sealed microfluidic device was then placed in a closed chamber (60 × 60 × 40 cm^3). The CO_2 concentration in the chamber was monitored by a CO_2 sensor. Bromo thymol blue aqueous solution (0.25 g/L) was first pumped through the microfluidic device by a syringe pump (TSE systems 540060). When the microfluidic device was filled with bromo thymol blue aqueous solution, the pumping was stopped, and ~32 g of dry ice was introduced and immediately evaporated in the closed chamber to give a CO_2 concentration of ~10%. This rapidly changed the solution color in the microfluidic from green to yellow, and then the

pumping started again, with flow rates varying from 25 µl/min, 50 µl/min, 100 µl/min, 200 µl/min to 400 µl/min (Video S5). When the flow rate was changed, the color of the flow reached a steady state after ~30 s. The images recorded at this stage were then extracted from the video and analyzed by Image J to calculate the acidic yellow area.

To check whether the transparent cover is permeable to CO_2, a microfluidic device printed only with the poly(ethylene glycol) diacrylate (Mw 250) resin was tested under the same condition (~10% CO_2). In this case, the color of solution in the microfluidic channel barely changed, indicating negligible CO_2 permeability of the cover (Video S6).

Oil absorption experiments: Four polymer cubes ($9.6\times9.6\times9.6\,mm^3$) based on the same monomer (butyl acrylate) but with different structures were printed: a non-porous cube, a nanoporous cube, a macroporous cube and a hierarchically macro-nano porous lattice with a macropore diameter of 0.9 mm. The nanoporous and macro-nano porous cubes were printed using an ink with porogens (BA-1: 30% wt% BA, 20 wt% EDMA and 50 wt% 1-decanol), while the non-porous cube and macroporous cube was printed using ink without porogens (60 wt% BA and 40 wt% EDMA). The absorbents were first weighed and completed immersed in the oil/water mixture for 2 minutes, and the weight was recorded again right after taking out from the oil/water mixture. The mass-based oil absorption capacity *k* was calculated from the following equation:

$$k = \frac{m_t - m_0}{m_0}$$

where m_t and m_0 are the total mass after immersion and the original mass of the absorbent, respectively.

References:

[1] T. Nishino, M. Meguro, K. Nakamae, M. Matsushita, Y. Ueda, *Langmuir* **1999**, 15, 4321.

[2] V. Liimatainen, M. Vuckovac, V. Jokinen, V. Sariola, M. J. Hokkanen, Q. Zhou, R. H. A. Ras, *Nat. Commun.* **2017**, 8, 1798.

[3] H. Gong, M. Beauchamp, S. Perry, A. T. Woolley, G. P. Nordin, *RSC Adv.* **2015**, 5, 106621.

[4] A. Urrios, C. Parra-Cabrera, N. Bhattacharjee, A. M. Gonzalez-Suarez, L. G. Rigat-Brugarolas, U. Nallapatti, J. Samitier, C. A. DeForest, F. Posas, J. L. Garcia-Cordero, A. Folch, *Lab Chip* **2016**, 16, 2287.

[5] H. Gong, B. P. Bickham, A. T. Woolley, G. P. Nordin, *Lab Chip* **2017**, 17, 2899.

Video S1 Water droplet moving freely on 3D-printed complex-shaped structures

Video S2 3D-printed superhydrophobic cube ($10 \times 10 \times 10$ mm^3) supporting a mass of 1 kg

Video S3 Water droplets bouncing and rolling on the external and internal surface of a 3D printed superhydrophobic bowl

Video S4 Water droplet moving freely in a 3D-printed superhydrophobic microfluidic channel

Video S5 CO_2 permeation through 3D-printed porous superhydrophobic microfluidic device

Video S6 3D-printed non-porous microfluidic device placed in CO_2 environment

Video S7 Oil permeation into a 3D-printed superhydrophobic cube

Video S8 Oil absorption of a 3D-printed hierarchical macro-nano porous superhydrophobic cube